Highly Reactive Atomic Hydrogen as an Alternative Reactant for Atomic Layer Deposition of Platinum Using $MeCpPtMe_3$

Authors
Van Bui, Hao; Grillo, Fabio; Nguyen, Dieu Minh; Dang, Manh Duc; Aarnink, Antonius A.I.; Wolters, Rob A.M.; van Ommen, J. Ruud; Kovalgin, Alexey Y.

DOI
10.1021/acs.jpcc.5c03286

Publication date
2025

Document Version
Final published version

Published in
Journal of Physical Chemistry C

Citation (APA)
Van Bui, H., Grillo, F., Nguyen, D. M., Dang, M. D., Aarnink, A. A. I., Wolters, R. A. M., van Ommen, J. R., & Kovalgin, A. Y. (2025). Highly Reactive Atomic Hydrogen as an Alternative Reactant for Atomic Layer Deposition of Platinum Using $MeCpPtMe_3$. *Journal of Physical Chemistry C*, *129*(30), 13822-13829. https://doi.org/10.1021/acs.jpcc.5c03286

THE JOURNAL OF PHYSICAL CHEMISTRY C
A JOURNAL OF THE AMERICAN CHEMICAL SOCIETY

pubs.acs.org/JPCC

Article

Highly Reactive Atomic Hydrogen as an Alternative Reactant for Atomic Layer Deposition of Platinum Using $MeCpPtMe_3$

Hao Van Bui,* Fabio Grillo, Dieu Minh Nguyen, Manh Duc Dang, Antonius A. I. Aarnink, Rob A. M. Wolters, J. Ruud van Ommen, and Alexey Y. Kovalgin

Cite This: *J. Phys. Chem. C* 2025, 129, 13822−13829

Read Online

ACCESS | Metrics & More | Article Recommendations | Supporting Information

ABSTRACT: Atomic layer deposition (ALD) of platinum (Pt) has gained significant interest in the recent years due to its capability of depositing various Pt nanostructures for applications in different fields, such as Pt nanoparticles (NPs) for catalytic reactions and energy devices and Pt thin films for microelectronic technology. Among various developed processes, Pt ALD using $MeCpPtMe_3$ as the precursor has been most popularly employed owing to the high reactivity, volatility, and thermal stability of the precursor, which enable controlled deposition of Pt nanostructures in a broad range of temperatures. Typical $MeCpPtMe_3$-based Pt ALD processes use O_2 and H_2 as the coreactants. In this study, we explore atomic hydrogen as an alternative and reveal its exceptional reactivity that outperforms H_2 and O_2. Specifically, atomic hydrogen enables the deposition of highly dispersed Pt NPs with narrow particle size distributions (i.e., standard deviation <0.3 nm) on various oxide surfaces, including TiO_2, SiO_2, CeO_2 and V_2O_5, which is unattainable with H_2 under identical experimental conditions. In addition, it facilitates the deposition of Pt NPs with improved size uniformity and accelerates the closure of Pt films compared to ALD processes using O_2 as the coreactant. The results demonstrate a significant potential of atomic hydrogen as a highly effective coreactant for ALD of Pt NPs and thin films.

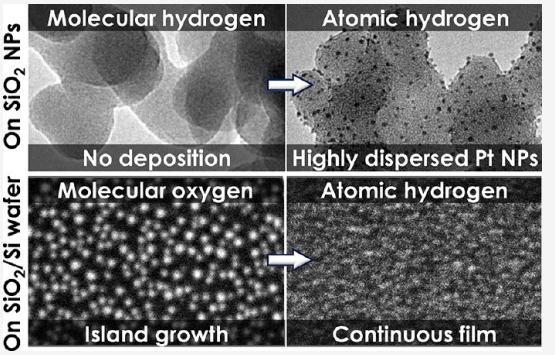

INTRODUCTION

Platinum (Pt) is a noble metal known for its exceptional catalytic activity,[1,2] low electrical resistivity,[3,4] and high thermal stability.[5,6] These distinctive properties make Pt suitable for a wide range of applications, including catalysis,[7,8] fuel cells,[9,10] and advanced electronics.[11,12] In catalysis, Pt is often utilized as nanoparticles (NPs) on high-surface-area supports to maximize the active surface area while minimizing the Pt usage.[13,14] Therefore, atomic layer deposition (ALD) has been extensively employed for depositing Pt NPs due to its ability to control the particle size at the atomic level, which is enabled by the self-limiting surface reactions in ALD.[15−17]

Pt ALD processes using $MeCpPtMe_3$ as the precursor typically employ oxygen (O_2),[18,19] ozone (O_3),[20,21] or molecular hydrogen (H_2)[22,23] as the coreactants. The oxygen-based processes using O_2 or O_3 provide high reactivity with $MeCpPtMe_3$, resulting in more efficient deposition.[22,24] In addition, these processes are highly effective on a wide range of substrates, such as oxides,[18,25,26] nanocarbon,[14,27] and polymers.[28] However, the use of oxygen can lead to platinum oxide formation, especially at low temperatures.[29] In contrast, hydrogen enables the deposition of Pt with a higher purity.[22] A disadvantage of using H_2 is, however, its limited reactivity for the removal of the precursor ligands. In addition, the H_2-based ALD processes often result in an incubation period or poor nucleation. This limitation restricts the effectiveness of H_2-based ALD of Pt, particularly on noncatalytic or inert substrates.

Atomic hydrogen has been demonstrated as an excellent coreactant that effectively facilitates the ligand removal, surface reduction, and enhanced nucleation in ALD of metals such as Mo,[30] W,[31,32] and Cu.[33] Yao et al. found that H_2 was ineffective in removing precursor ligands in ALD of Cu using Cu(I)-*sec*-butyl-2-iminopyrrolidinate (Cu(I)-sBu-IP) and Cu-(I)-2-(*tert*-butylimino)-5,5-dimethyl-pyrrolidinate (Cu(I)-*t*Bu-IDMP).[33] However, the use of atomic hydrogen not only effectively removed the ligands from the surface and but also reduced Cu(I) oxide to its metallic state. Similarly, van der Zouw et al. reported that in ALD of Mo using $MoCl_2O_2$ as the precursor, atomic hydrogen mitigated the nucleation delay, extended the deposition temperature range, and enabled Mo film growth on various substrates, including Si, SiO_2, Si_3N_4, SiC, Al_2O_3, HfO_2, and SiOC.[30] Most recently, using density

Received: June 1, 2025
Revised: July 8, 2025
Accepted: July 10, 2025
Published: July 17, 2025

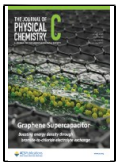

https://doi.org/10.1021/acs.jpcc.5c03286
J. Phys. Chem. C 2025, 129, 13822−13829

functional theory (DFT) calculations, Ta et al. compared the removal efficiency of $MeCpPtMe_3$ ligands by H_2, O_2 and atomic hydrogen during the Pt ALD processes.[34] The calculation of reaction and activation energies for ligand removal by each coreactant revealed a superior performance of atomic hydrogen over the other two coreactants. In particular, removing one of the CH_3 groups from the $MeCpPtMe_3$ precursor requires an activation energy of 1.83 eV with O_2 and 1.94 eV with H_2, primarily due to the energy needed to dissociate these molecules. In contrast, the removal by atomic hydrogen is mostly barrierless and spontaneous.[34] In addition, atomic hydrogen is found to be more effective in removing the MeCp ligand than H_2 and O_2. These studies demonstrate a great potential of atomic hydrogen as an efficient coreactant for metal ALD.

In this work, we experimentally validate the advantages of atomic hydrogen as a coreactant for Pt ALD using $MeCpPtMe_3$. Atomic hydrogen is generated by using hot-wire technology,[35,36] and the deposition is examined on various oxide surfaces, including TiO_2, SiO_2, CeO_2, and V_2O_5. We demonstrate that atomic hydrogen enables highly uniform deposition of Pt NPs with narrow particle size distributions (PSDs) and standard deviations smaller than 0.3 nm across all surfaces. In contrast, molecular hydrogen under similar experimental conditions results in virtually no Pt deposition. Additionally, atomic hydrogen outperforms O_2 in facilitating the faster film closure when deposited on Si/SiO_2 wafers as well as the deposition of Pt NPs with improved size uniformity. Our results reveal a substantial potential of atomic hydrogen as a highly effective coreactant for Pt ALD, which can be extended to ALD of other metals.

METHODS

Chemicals, Materials, and Substrates. The Pt precursor $MeCpPtMe_3$ (purity ≥98%) contained in a stainless steel bubbler was obtained from Strem Chemicals and used as received. During the deposition, the bubbler was maintained at 70 °C via a heating jacket, while the line connecting the bubbler to the reactor was kept at 80 °C to prevent condensation of the precursor.

The oxide nanopowders used in this work, including TiO_2, SiO_2, CeO_2 and V_2O_5, were obtained from Evonik. The nanopowder was first dispersed and crashed in an agate mortar in ethanol, which was subsequently loaded onto a transmission electron microscopy (TEM) grid (aluminum grid, QUANTI-FOIL R 1.2/1.3 type, 3.05 mm in diameter) by drop-casting. The same procedure was applied for every powder. The TEM grids loaded with the nanopowders were used as the substrates for studying the deposition of Pt on different oxide surfaces. For the deposition on flat substrates, 4-in. Si wafers with 100 nm-thick thermally grown SiO_2 were used. Prior to the deposition, the wafers were cleaned by a stadard cleaning process.

Generation and Verification of Atomic Hydrogen. Atomic hydrogen was generated by hot-wire technology, in which a hydrogen flow was passed through a hot W-filament before entering to the reactor. At high temperatures, molecular hydrogen molecules were dissociated into atomic hydrogen. The presence of atomic hydogen was verified by the eching of tellurium (Te) films. The experimental apparatus, the filament temperature determination methods, the generation and verification of the presence of atomic hydrogen are described in detail in other studies.[35−37] In this work, the filament was maintained at 1750 °C and a constant H_2 flow of 25 sccm was used.

ALD of Platinum. The deposition of Pt was conducted in a home-built single-wafer ALD system equipped with a hot-wire module for the generation of atomic hydrogen, as described elsewhere.[35,36] Briefly, the system consisted of two reactors (i.e., inner and outer). The volume of the inner reactor where the substrate was located was 25 cm^3. The hot-wire module was mounted on the inner reactor, positioned a few centimeters above the wafer surface in such a way that there was no direct line-of-sight between the filament and the substrate to ensure that its temperature did not affect the sample.

For the deposition on oxide nanoparticles, the TEM grids loaded with oxide nanopowders (TiO_2, SiO_2, CeO_2, and V_2O_5) were immobilized on top of a dummy Si wafer and transferred into the reactor via a load-lock. Prior to every deposition, the reactor was evacuated to a base pressure of $\sim 5 \times 10^{-6}$ mbar. The reactor allowed for controlling the pressure inside the reactor by adjusting the opening of the throttle valve between the reactor and the turbo pump. This enabled our study of the deposition at different pressures. For all experiments, the Pt precursor $MeCpPtMe_3$ exposure time was fixed at 5 s, whereas exposure time of the coreactant gas was fixed at 300 s. All the depositions were conducted at 300 °C. We note that the experimental apparatus is designed in such a way that the wafer is well screened from the thermal radiation generated by the hot filament. Therefore, the influence of the filament on the substrate temperature is negligible.

An ALD cycle consisted of 8 steps, including four pumping steps to control the pressure inside the reactor during the deposition, which are commonly not used in conventional ALD processes. In the first step, the reactor was evacuated to a pressure of 5×10^{-6} mbar (step 1). Next, the Pt precursor was introduced into the reactor for 5 s (step 2). During this step, the vapor pressure of the precursor in the bubbler varied slightly in the range between 1.0 and 1.2 mbar, whereas the pressure inside the reactor was in the range of $3.0-5.0 \times 10^{-5}$ mbar. After the precursor pulse, the reactor was evacuated again to the pressure of 5×10^{-6} mbar (step 3), followed by purging with a constant N_2 flow of 50 sccm for 10 s (step 4). Next, the reactor was evacuated to the pressure of 5×10^{-6} mbar (step 5) before introducing the coreactant (H_2, H or O_2) into the reactor for 300 s under a constant gas flow of 25 sccm (step 6). Such a long exposure time was needed to ensure that the reactions were in the saturation regime. During this step, the partial pressure of the coreactant was controlled by adjusting the opening of the throttle valve between the reactor and the turbo pump. Thereafter, the reactor was evacuated once more to the pressure of 5×10^{-6} mbar (step 7), which was eventually purged by N_2 for 30 s with a constant N_2 flow of 50 sccm in the last step (step 8). The evacuation in steps 3 and 7 as well as the long purge time in steps 4 and 8 were to ensure no CVD contribution to the deposition. The total time for each ALD cycle was approximately 600 s.

Materials Characterization and Analysis. Transmission electron microscopy (TEM) images of the samples were taken using a JEOL JEM1400 transmission electron microscope operated at 120 kV. The number-based particle size distributions of the Pt NPs were obtained by measuring the projected diameter of the NPs manually using Gatan Digital Micrograph software (Version 2.31.734.0). Field-emission scanning electron microscopy (FE-SEM) images of the

https://doi.org/10.1021/acs.jpcc.5c03286
J. Phys. Chem. C 2025, 129, 13822−13829

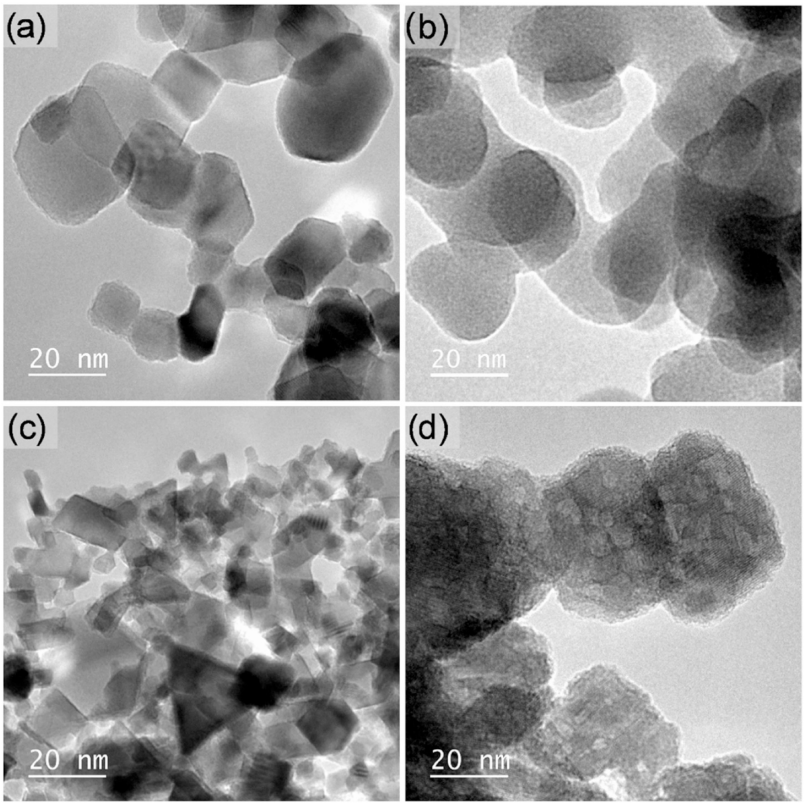

Figure 1. TEM images of the oxide surfaces after 5 ALD cycles using H_2 at 300 °C and 1 mbar: TiO_2 (a), SiO_2 (b), CeO_2 (c), and V_2O_5 (d).

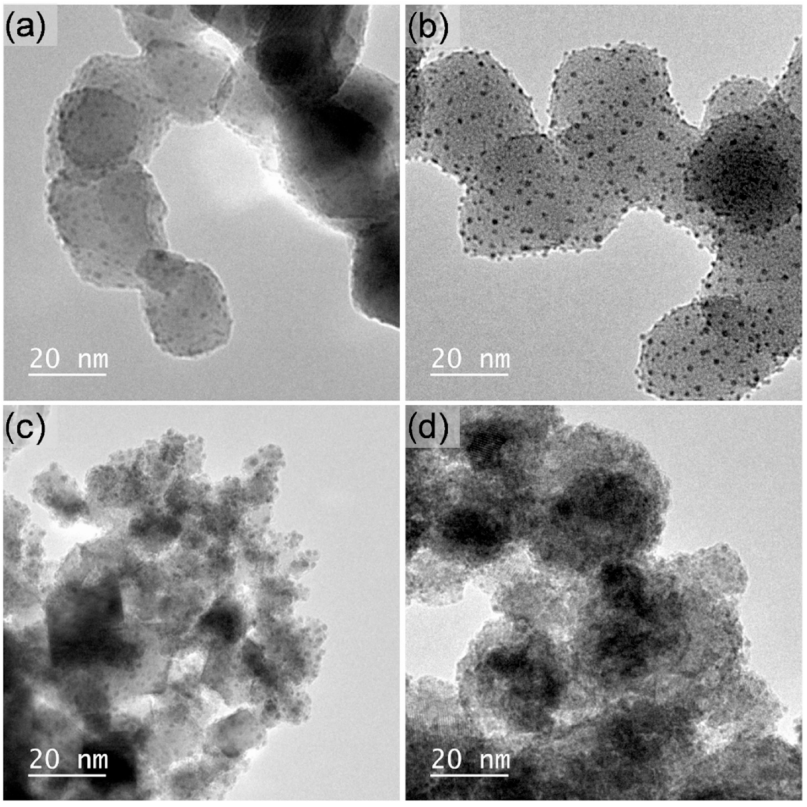

Figure 2. TEM images of Pt NPs deposited by ALD using atomic hydrogen on different oxide surfaces after 5 ALD cycles at 300 °C with the coreactant partial pressure of 1 mbar: TiO_2 (a), SiO_2 (b), CeO_2 (c), and V_2O_5 (d).

samples were obtained using a Zeiss Merlin high-resolution FE-SEM system with a point resolution of 1.2 nm. The images were acquired at a magnification of 500 K under an electron high tension (EHT) voltage of 1.4 kV.

https://doi.org/10.1021/acs.jpcc.5c03286
J. Phys. Chem. C 2025, 129, 13822−13829

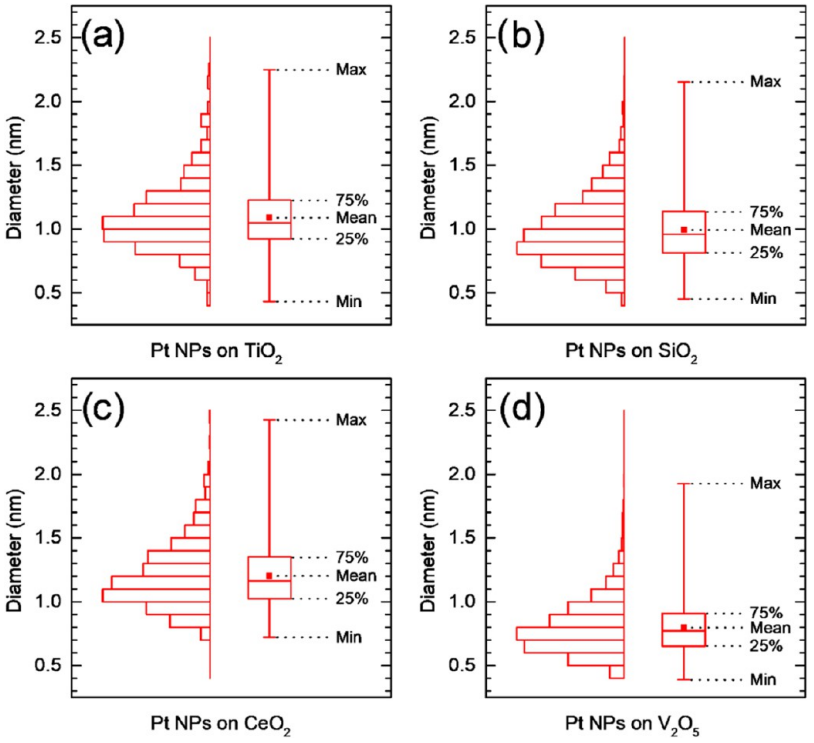

Figure 3. PSDs of Pt NPs deposited by ALD using atomic hydrogen on different oxide surfaces after 5 ALD cycles at 300 °C with the coreactant partial pressure of 1 mbar: TiO_2 (a), SiO_2 (b), CeO_2 (c), and V_2O_5 (d).

RESULTS AND DISCUSSION

ALD of Platinum Using $MeCpPtMe_3$ and H_2. Figures 1 and S1 (Supporting Information (SI)) show TEM images of the oxide nanopowders (TiO_2, SiO_2, CeO_2 and V_2O_5) after 5 cycles of Pt ALD at 300 °C using H_2 as the coreactant with an H_2 partial pressure of 1 mbar. The results show that no trace of the Pt NPs is found on any of the surfaces. As we will show later, the ALD process using O_2 and atomic hydrogen resulted in a substantial deposition of Pt NPs on TiO_2 after the same number of ALD cycles at the same temperature and coreactant partial pressure. The absence of Pt NPs when using H_2 as the coreactant indicates the lower efficiency of H_2 in the removal of the precursor ligands. This is consistent with the findings reported by Gould et al.,[22,38,39] who observed that the Pt loading obtained for the O_2-based ALD process was significantly higher than that of the H_2 counterpart for the same $MeCpPtMe_3$ exposure.

ALD of Pt Using Atomic Hydrogen and O_2. For the same $MeCpPtMe_3$ exposure, the ALD process at 300 °C and 1 mbar using atomic hydrogen as the coreactant enables a substantial deposition of Pt NPs on all surfaces. TEM images of Pt NPs on TiO_2, SiO_2, CeO_2, and V_2O_5 after 5 ALD cycles are presented in Figures 2 and S2 (SI), indicating a uniform distribution of highly dispersed Pt NPs across the entire surface of the oxide nanoparticles. The particle size distributions (PSDs) of Pt NPs on different surfaces are presented in Figure 3. Each figure includes a histogram of the PSD (left) and a box-and-whisker plot (right). The whiskers represent the range from the minimum to maximum sizes, while the box indicates the range from the 25th to the 75th percentile of the distribution. The mean diameters of Pt NPs, indicated by the solid squares in the boxes, are in the range between 0.8 and 1.1 nm, whereas the standard deviations of Pt NPs are in between 0.21 and 0.26 nm, as presented in Table 1.

Table 1. Average Particle Size and Standard Deviation of Pt NPs Deposited on Different Oxide Nanopowders Using Atomic Hydrogen as the Co-Reactant

materials	mean diameter (nm)	standard deviation (nm)
Pt/TiO_2	1.1	0.26
Pt/SiO_2	1.0	0.26
Pt/CeO_2	1.2	0.25
Pt/V_2O_5	0.8	0.21

The results indicate that the mean sizes of Pt NPs deposited on different surfaces are comparable. The small standard deviations quantitatively characterize the narrow PSDs achieved by the atomic hydrogen ALD process, which is attractive for e.g., catalystic applications. Remarkably, the PSD of Pt NPs deposited on TiO_2 with atomic hydrogen (Figure 3a) is significantly narrower than that obtained for the O_2-based ALD process, as demonstrated in Figures 4 and S3 (SI). For the latter, the mean diameter and the standard deviation of Pt NPs are 1.3 and 0.92 nm, respectively. The significantly larger standard deviation indicates a high degree of nonuniformity in particle size, as evidenced by the TEM image. This observation suggests that atomic hydrogen effectively suppresses the coarsening of Pt NPs, a phenomenon commonly observed in Pt ALD using $MeCpPtMe_3$ and O_2.[40,41]

ALD of Pt on SiO_2/Si Wafers. For most applications in electronic devices, continuous Pt films are highly desirable to achieve high conductivity.[26] However, when deposited on oxide surfaces, such as Al_2O_3,[42] SiO_2,[43] TiO_2,[44] and $SrTiO_3$,[45] Pt ALD follows the island-growth mode, which requires a large number of ALD cycles to achieve a continuous film. For example, Christensen et al.[45] reported that on $SrTiO_3$ substrate, the Pt film closure occurred after 40 ALD cycles, while Lee et al.[28] observed a 100% coverage of Pt on SiO_2/Si

https://doi.org/10.1021/acs.jpcc.5c03286
J. Phys. Chem. C 2025, 129, 13822−13829

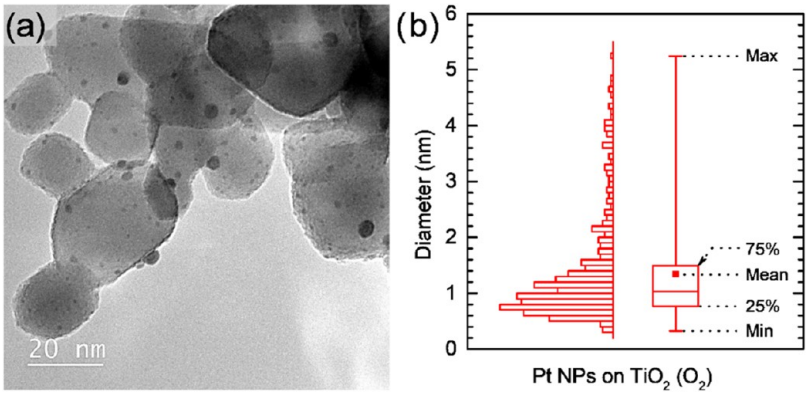

Figure 4. TEM image (a) and the corresponding PSD of Pt NPs (b) deposited on TiO_2 by ALD using O_2 at 300 °C with O_2 partial pressure of 1 mbar after 5 ALD cycles.

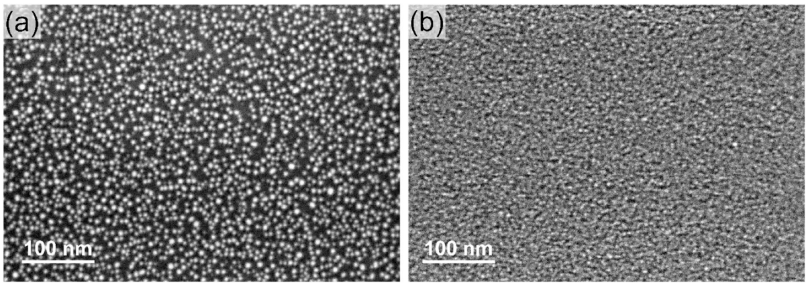

Figure 5. SEM images of Pt deposited on SiO_2/Si wafers at 300 °C with the coreactant partial pressure of 1 mbar for 25 ALD cycles by ALD using O_2 (a) and atomic hydrogen (b).

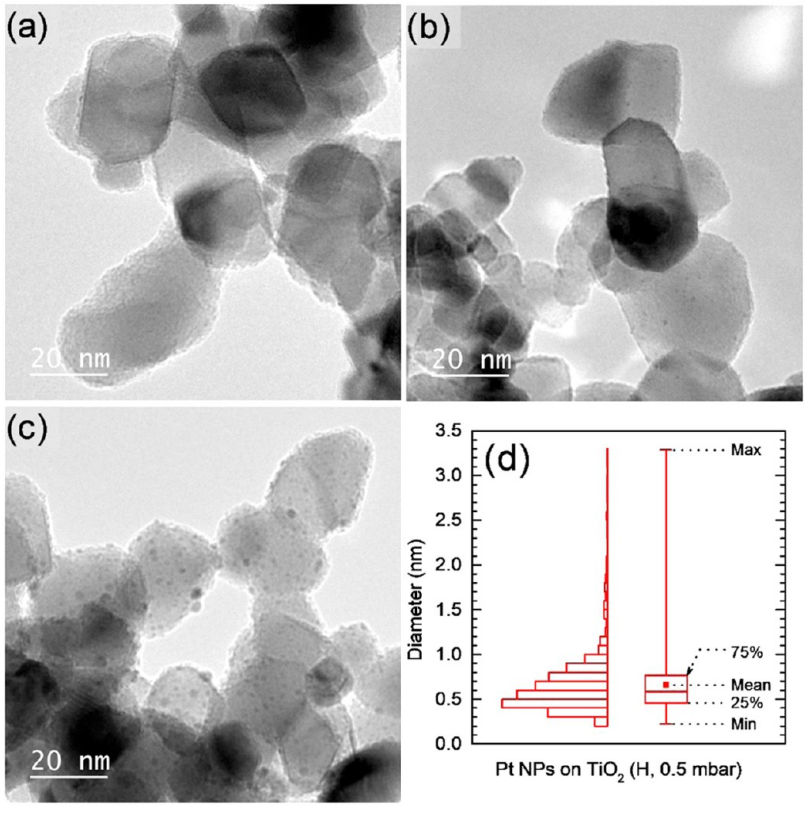

Figure 6. TEM images TiO_2 nanoparticles after 5 ALD cycles at 300 °C and coreactant partial pressure of 0.5 mbar using H_2 (a), O_2 (b), and atomic hydrogen (c). Figure d shows the PSD of Pt NPs deposited by the process using atomic hydrogen.

https://doi.org/10.1021/acs.jpcc.5c03286
J. Phys. Chem. C 2025, 129, 13822−13829

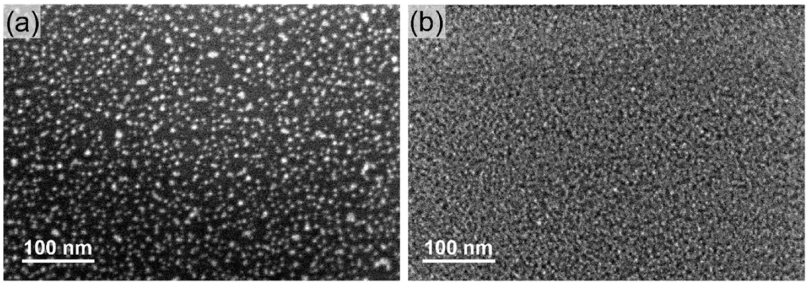

Figure 7. SEM images of Pt deposited on SiO_2/Si wafers at 300 °C with the coreactant partial pressure of 0.5 mbar for 25 ALD cycles by ALD using O_2 (a) and atomic hydrogen (b).

substrate only after 400 ALD cycles. To enhance the nucleation and achieve continuous films with fewer ALD cycles, surface pretreatment of the substrate is often applied. This can be done by exposing the substrate to plasmas,[46] or to chemicals such as trimethylaluminum (TMA),[47] NH_3,[48] or precleaning the substrate in piranha solution prior to ALD.[44]

To explore the potential in ALD of continuous Pt films for microelectronic devices, the deposition of Pt on SiO_2/Si wafers by ALD using atomic hydrogen was conducted. For a comparison, the ALD process using O_2 as the coreactant was also carried out under identical experimental conditions. Figure 5 presents SEM images of the Pt deposited on SiO_2/Si substrates at 300 °C with the coreactant partial pressure of 1 mbar using O_2 (Figure 5a) and atomic hydrogen (Figure 5b). The O_2-based ALD process results in the deposition of discrete Pt NPs after 25 ALD cycles, indicating the island-growth mode commonly observed for the thermal ALD of Pt on oxide surfaces using either O_2 or O_3.[20,28,43] Remarkably, for the same number of ALD cycles the ALD process using atomic hydrogen results in a closed Pt film (i.e., film closure, Figure 5b). The SEM image in Figure 5b also indicates that the nucleus density obtained by the atomic hydrogen process is substantially higher than that obtained by the O_2-based ALD process, Notably, a previous study of van der Zouw et al. demonstrated that the use of atomic hydrogen as the coreactant completely diminished the nucleation delay in the thermal ALD of Mo on a variety of oxide and nitride substrates.[30] Hence, it can be concluded that atomic hydrogen strongly enhances the nucleation of Pt on the SiO_2 surface, which may arise from the generation of a high density of active sites on the surface through its interaction with the substrate.

ALD of Pt at a lower coreactant partial pressure. Previous studies demonstrated that O_2 partial pressure strongly influenced the nucleation and growth of Pt NPs in ALD using $MeCpPtMe_3$ and O_2.[49,50] Mackus et al. observed that Pt ALD on Al_2O_3 conducted at low O_2 partial pressures (a few mTorr) did not yield any Pt growth, even after extended deposition of up to 1000 ALD cycles.[50] At an increased O_2 partial pressure of 0.1 Torr, Pt growth was achieved but with a considerable nucleation delay of approximately 160 cycles. This nucleation delay decreased rapidly with further increases in the O_2 partial pressure. The results from our Pt ALD on TiO_2 NPs at a coreactant partial pressure of 0.5 mbar (i.e., ~0.375 Torr) using H_2, O_2 and atomic hydrogen are presented in Figures 6a–c and S4. Similar to the process at 1 mbar, no deposition of Pt is achieved for ALD using H_2 after 5 ALD cycles (Figure 6a). At the same time, ALD using O_2 results in ultrasmall Pt NPs sporadically distributed on the TiO_2 surface (Figure 6b). This reflects the effect of O_2 partial pressure on the deposition of Pt. However, when atomic hydrogen is used, a substantial deposition of Pt NPs is achieved (Figure 6c), indicating the better performance of atomic hydrogen with respect to H_2 and O_2 at the lower pressure. Nevertheless, a pronounced effect of partial pressure on the deposition of Pt NPs is also observed for atomic hydrogen. The PSD of Pt NPs deposited at the partial pressure of 0.5 mbar (Figure 6d) shows a broader distribution. The mean diameter of Pt NPs is found to be 0.7 nm with a standard deviation of 0.35 nm. The smaller particle size with the larger standard deviation compared to those achieved by the deposition at 1 mbar suggests the higher nonuniformity of the Pt NP size at the lower particle pressure. Such an effect was previously observed for the Pt ALD process using O_2.[49] The decreased uniformity in particle size at the lower partial pressure can be attributed to the slower ligand removal rate due to the lower coreactant concentration, which consequently facilitates the diffusion and coalescence of Pt NPs.

The deposition of Pt on SiO_2/Si substrates at the coreactant partial pressure of 0.5 mbar is shown Figure 7. The O_2-based ALD process results in Pt NPs (Figure 7a) similar to the deposition at 1 mbar, however, with a lower uniformity in particle size. Notably, a closure of the Pt film is also achieved for the ALD process using atomic hydrogen at this pressure (Figure 7b). These results once again indicate that atomic hydrogen can accelerate the closure of Pt films in ALD using $MeCpPtMe_3$ as the Pt precursor, demonstrating its great potential for application in microelectronic technology.

CONCLUSIONS

In conclusion, by conducting experiments of ALD using $MeCpPtMe_3$ as the precursor in combination with H_2, O_2 or atomic hydrogen as the coreactant, our work demonstrates the excellent performance of atomic hydrogen for ALD of Pt NPs and thin films. The use of atomic hydrogen enables the deposition of highly dispersed Pt NPs with narrow PSDs (standard deviation <0.3 nm) on different oxide surfaces, i.e., TiO_2, SiO_2, CeO_2, and V_2O_5, which cannot be achieved by using molecular hydrogen under identical experimental conditions. This is highly relevant for catalytic applications. In addition, it enables the deposition of Pt NPs with higher size uniformity than that of the O_2-based process. Importantly, atomic hydrogen enhances the nucleation of Pt on Si/SiO_2 substrate, thereby accelerating the film closure, which is desirable for applications in semiconductor technology. Our findings indicate that atomic hydrogen is highly reactive for precursor ligand removal and strongly affects the nucleation of Pt, which may pave the way for broader applications of atomic hydrogen in ALD of Pt and other metals.

https://doi.org/10.1021/acs.jpcc.5c03286
J. Phys. Chem. C 2025, 129, 13822−13829

■ ASSOCIATED CONTENT

Supporting Information

The Supporting Information is available free of charge at https://pubs.acs.org/doi/10.1021/acs.jpcc.5c03286.

TEM images of the oxide nanoparticles after 5 cycles of Pt ALD using H_2 at the partial pressure of 1 mbar (Figure S1); TEM images of Pt NPs deposited by ALD using atomic hydrogen at the partial pressure of 1 mbar on different oxide surfaces after 5 cycles (Figure S2); TEM images of Pt NPs deposited on TiO_2 by ALD using O_2 at the partial pressure of 1 mbar (Figure S3); TEM images of TiO_2 nanoparticles after 5 cycles of Pt ALD using H_2, O_2 and atomic hydrogen at the coreactant partial pressure of 0.5 mbar (Figure S4) (PDF)

■ AUTHOR INFORMATION

Corresponding Author

Hao Van Bui − *Faculty of Materials Science and Engineering, Phenikaa University, Hanoi 12116, Vietnam;* orcid.org/0000-0001-8460-1409; Email: hao.buivan@phenikaa-uni.edu.vn

Authors

Fabio Grillo − *Department of Chemical Engineering, Delft University of Technology, Delft 2629 HZ, The Netherlands*

Dieu Minh Nguyen − *Faculty of Materials Science and Engineering, Phenikaa University, Hanoi 12116, Vietnam*

Manh Duc Dang − *Faculty of Materials Science and Engineering, Phenikaa University, Hanoi 12116, Vietnam*

Antonius A. I. Aarnink − *MESA+ Institute for Nanotechnology, University of Twente, Enschede 7500 AE, The Netherlands*

Rob A. M. Wolters − *MESA+ Institute for Nanotechnology, University of Twente, Enschede 7500 AE, The Netherlands*

J. Ruud van Ommen − *Department of Chemical Engineering, Delft University of Technology, Delft 2629 HZ, The Netherlands;* orcid.org/0000-0001-7884-0323

Alexey Y. Kovalgin − *MESA+ Institute for Nanotechnology, University of Twente, Enschede 7500 AE, The Netherlands;* orcid.org/0000-0001-7418-7734

Complete contact information is available at: https://pubs.acs.org/10.1021/acs.jpcc.5c03286

Notes

The authors declare no competing financial interest.

■ ACKNOWLEDGMENTS

This work is funded by Phenikaa Innovation Foundation (Phenikaa Group), under the grant number ĐMST.2022.03.

■ REFERENCES

(1) Li, M.; Duanmu, K.; Wan, C.; Cheng, T.; Zhang, L.; Dai, S.; Chen, W.; Zhao, Z.; Li, P.; Fei, H.; et al. Single-Atom Tailoring of Platinum Nanocatalysts for High-Performance Multifunctional Electrocatalysis. *Nat. Catal.* **2019**, *2* (6), 495−503.

(2) Hansen, J. N.; Prats, H.; Toudahl, K. K.; Mørch Secher, N.; Chan, K.; Kibsgaard, J.; Chorkendorff, I. Is There Anything Better than Pt for HER? *ACS Energy Lett.* **2021**, *6* (4), 1175−1180.

(3) Lee, W.-J.; Wan, Z.; Kim, C.-M.; Oh, I.-K.; Harada, R.; Suzuki, K.; Choi, E.-A.; Kwon, S.-H. Atomic Layer Deposition of Pt Thin Films Using Dimethyl (N,N-Dimethyl-3-Butene-1-Amine-N) Platinum and O_2 Reactant. *Chem. Mater.* **2019**, *31* (14), 5056−5064.

(4) Kim, H. J. K.; Kaplan, K. E.; Schindler, P.; Xu, S.; Winterkorn, M. M.; Heinz, D. B.; English, T. S.; Provine, J.; Prinz, F. B.; Kenny, T. W. Electrical Properties of Ultrathin Platinum Films by Plasma-Enhanced Atomic Layer Deposition. *ACS Appl. Mater. Interfaces* **2019**, *11* (9), 9594−9599.

(5) Porsgaard, S.; Merte, L. R.; Ono, L. K.; Behafarid, F.; Matos, J.; Helveg, S.; Salmeron, M.; Cuenya, B. R.; Besenbacher, F. Stability of Platinum Nanoparticles Supported on SiO2/Si(111): A High-Pressure X-Ray Photoelectron Spectroscopy Study. *ACS Nano* **2012**, *6* (12), 10743−10749.

(6) Ono, L. K.; Yuan, B.; Heinrich, H.; Cuenya, B. R. Formation and Thermal Stability of Platinum Oxides on Size-Selected Platinum Nanoparticles: Support Effects. *J. Phys. Chem. C* **2010**, *114* (50), 22119−22133.

(7) Chen, A.; Holt-Hindle, P. Platinum-Based Nanostructured Materials: Synthesis, Properties, and Applications. *Chem. Rev.* **2010**, *110* (6), 3767−3804.

(8) Liu, D.; Li, X.; Chen, S.; Yan, H.; Wang, C.; Wu, C.; Haleem, Y. A.; Duan, S.; Lu, J.; Ge, B.; et al. Atomically Dispersed Platinum Supported on Curved Carbon Supports for Efficient Electrocatalytic Hydrogen Evolution. *Nat. Energy* **2019**, *4* (6), 512−518.

(9) Lee, W.-J.; Bera, S.; Shin, H.-C.; Hong, W.-P.; Oh, S.-J.; Wan, Z.; Kwon, S.-H. Uniform and Size-Controlled Synthesis of Pt Nanoparticle Catalyst by Fluidized Bed Reactor Atomic Layer Deposition for PEMFCs. *Adv. Mater. Interfaces* **2019**, *6* (21), No. 1901210.

(10) Jung, N.; Chung, D. Y.; Ryu, J.; Yoo, S. J.; Sung, Y.-E. Pt-Based Nanoarchitecture and Catalyst Design for Fuel Cell Applications. *Nano Today* **2014**, *9* (4), 433−456.

(11) Mackus, A. J. M.; Dielissen, S. A. F.; Mulders, J. J. L.; Kessels, W. M. M. Nanopatterning by Direct-Write Atomic Layer Deposition. *Nanoscale* **2012**, *4* (15), 4477−4480.

(12) Schlitz, R.; Amusan, A. A.; Lammel, M.; Schlicht, S.; Tynell, T.; Bachmann, J.; Woltersdorf, G.; Nielsch, K.; Goennenwein, S. T. B.; Thomas, A. Spin-Hall-Active Platinum Thin Films Grown via Atomic Layer Deposition. *Appl. Phys. Lett.* **2018**, *112* (24), No. 242403.

(13) Van Bui, H.; Grillo, F.; Kulkarni, S. S.; Bevaart, R.; Thang, N. V.; van der Linden, B.; Moulijn, J. A.; Makkee, M.; Kreutzer, M. T.; van Ommen, J. R. Low-Temperature Atomic Layer Deposition Delivers More Active and Stable Pt-Based Catalysts. *Nanoscale* **2017**, *9* (30), 10802−10810.

(14) Lee, W.-J.; Bera, S.; Kim, C. M.; Koh, E.-K.; Hong, W.-P.; Oh, S.-J.; Cho, E.; Kwon, S.-H. Synthesis of Highly Dispersed Pt Nanoparticles into Carbon Supports by Fluidized Bed Reactor Atomic Layer Deposition to Boost PEMFC Performance. *NPG Asia Mater.* **2020**, *12* (1), No. 40.

(15) Lu, J.; Elam, J. W.; Stair, P. C. Atomic Layer Deposition—Sequential Self-Limiting Surface Reactions for Advanced Catalyst "Bottom-up" Synthesis. *Surf. Sci. Rep.* **2016**, *71* (2), 410−472.

(16) Van Bui, H.; Grillo, F.; Van Ommen, J. R. Atomic and Molecular Layer Deposition: Off the Beaten Track. *Chem. Commun.* **2017**, *53* (1), 45−71.

(17) Dinh, K.-H. T.; Ta, H. T. T.; Nguyen, N. L.; Le, V. T.; Nguyen, V. H.; Van Bui, H. Dimension Control of Platinum Nanostructures by Atomic Layer Deposition: From Surface Chemical Reactions to Applications. *Chem. Mater.* **2023**, *35* (6), 2248−2280.

(18) Aaltonen, T.; Ritala, M.; Sajavaara, T.; Keinonen, J.; Leskelä, M. Atomic Layer Deposition of Platinum Thin Films. *Chem. Mater.* **2003**, *15* (9), 1924−1928.

(19) Kessels, W. M. M.; Knoops, H. C. M.; Dielissen, S. a. F.; Mackus, A. J. M.; van de Sanden, M. C. M. Surface Reactions during Atomic Layer Deposition of Pt Derived from Gas Phase Infrared Spectroscopy. *Appl. Phys. Lett.* **2009**, *95* (1), No. 013114.

(20) Dendooven, J.; Ramachandran, R. K.; Devloo-Casier, K.; Rampelberg, G.; Filez, M.; Poelman, H.; Marin, G. B.; Fonda, E.; Detavernier, C. Low-Temperature Atomic Layer Deposition of Platinum Using (Methylcyclopentadienyl)Trimethylplatinum and Ozone. *J. Phys. Chem. C* **2013**, *117* (40), 20557−20561.

(21) Lee, H.-B.-R.; Bent, S. F. Formation of Continuous Pt Films on the Graphite Surface by Atomic Layer Deposition with Reactive O_3. *Chem. Mater.* **2015**, *27* (19), 6802−6809.
(22) Gould, T. D.; Lubers, A. M.; Corpuz, A. R.; Weimer, A. W.; Falconer, J. L.; Medlin, J. W. Controlling Nanoscale Properties of Supported Platinum Catalysts through Atomic Layer Deposition. *ACS Catal.* **2015**, *5* (2), 1344−1352.
(23) Setthapun, W.; Williams, W. D.; Kim, S. M.; Feng, H.; Elam, J. W.; Rabuffetti, F. A.; Poeppelmeier, K. R.; Stair, P. C.; Stach, E. A.; Ribeiro, F. H.; et al. Genesis and Evolution of Surface Species during Pt Atomic Layer Deposition on Oxide Supports Characterized by in Situ XAFS Analysis and Water−Gas Shift Reaction. *J. Phys. Chem. C* **2010**, *114* (21), 9758−9771.
(24) Van Bui, H.; Nguyen, A. P.; Dang, M. D.; Dinh, T. D.; Kooyman, P. J.; Ommen, J. R. V. What Could Be the Low-Temperature Limit of Atomic Layer Deposition of Platinum Using MeCpPtMe3 and Oxygen? *Chem. Commun.* **2024**, *60* (95), 14045−14048.
(25) Zhou, Y.; King, D. M.; Liang, X.; Li, J.; Weimer, A. W. Optimal Preparation of Pt/TiO_2 Photocatalysts Using Atomic Layer Deposition. *Appl. Catal., B* **2010**, *101* (1), 54−60.
(26) Lee, H.-B.-R.; Pickrahn, K. L.; Bent, S. F. Effect of O_3 on Growth of Pt by Atomic Layer Deposition. *J. Phys. Chem. C* **2014**, *118* (23), 12325−12332.
(27) Liu, C.; Wang, C.-C.; Kei, C.-C.; Hsueh, Y.-C.; Perng, T.-P. Atomic Layer Deposition of Platinum Nanoparticles on Carbon Nanotubes for Application in Proton-Exchange Membrane Fuel Cells. *Small* **2009**, *5* (13), 1535−1538.
(28) Lee, J.; Yoon, J.; Kim, H. G.; Kang, S.; Oh, W.-S.; Algadi, H.; Al-Sayari, S.; Shong, B.; Kim, S.-H.; Kim, H.; et al. Highly Conductive and Flexible Fiber for Textile Electronics Obtained by Extremely Low-Temperature Atomic Layer Deposition of Pt. *NPG Asia Mater.* **2016**, *8* (11), e331.
(29) Mackus, A. J. M.; Garcia-Alonso, D.; Knoops, H. C. M.; Bol, A. A.; Kessels, W. M. M. Room-Temperature Atomic Layer Deposition of Platinum. *Chem. Mater.* **2013**, *25* (9), 1769−1774.
(30) van der Zouw, K.; van der Wel, B. Y.; Aarnink, A. A. I.; Wolters, R. A. M.; Gravesteijn, D. J.; Kovalgin, A. Y. Low-Resistivity Molybdenum Obtained by Atomic Layer Deposition. *J. Vac. Sci. Technol. A* **2023**, *41* (5), No. 052402.
(31) Yang, M.; Aarnink, A. A. I.; Schmitz, J.; Kovalgin, A. Y. Low-Resistivity α-Phase Tungsten Films Grown by Hot-Wire Assisted Atomic Layer Deposition in High-Aspect-Ratio Structures. *Thin Solid Films* **2018**, *646*, 199−208.
(32) Yang, M.; Aarnink, A. A. I.; Schmitz, J.; Kovalgin, A. Y. Inherently Area-Selective Hot-Wire Assisted Atomic Layer Deposition of Tungsten Films. *Thin Solid Films* **2018**, *649*, 17−23.
(33) Yao, Y.; Chen, B.; Zaera, F. On the Mechanism of the Atomic Layer Deposition of Cu Films on Silicon Oxide Surfaces: Activation Using Atomic Hydrogen and Three-Dimensional Growth. *Chem. Mater.* **2023**, *35* (5), 2155−2164.
(34) Ta, H. T. T.; Nguyen, N. L.; Tieu, A. K.; Van Bui, H. Spontaneous Reactions by Atomic Hydrogen − An Extraordinary Reactant for Atomic Layer Deposition of Platinum. *Chem. Mater.* **2025**, *37* (3), 964−974.
(35) Van Bui, H.; Kovalgin, A. Y.; Aarnink, A. A. I.; Wolters, R. A. M. Hot-Wire Generated Atomic Hydrogen and Its Impact on Thermal ALD in TiCl4/NH3 System. *ECS J. Solid State Sci. Technol.* **2013**, *2* (4), P149.
(36) Kovalgin, A. Y.; Yang, M.; Banerjee, S.; Apaydin, R. O.; Aarnink, A. A. I.; Kinge, S.; Wolters, R. A. M. Hot-Wire Assisted ALD: A Study Powered by In Situ Spectroscopic Ellipsometry. *Adv. Mater. Interfaces* **2017**, *4* (18), No. 1700058.
(37) Onnink, A. J.; Schmitz, J.; Kovalgin, A. Y. How Hot Is the Wire: Optical, Electrical, and Combined Methods to Determine Filament Temperature. *Thin Solid Films* **2019**, *674*, 22−32.
(38) Lubers, A. M.; Muhich, C. L.; Anderson, K. M.; Weimer, A. W. Mechanistic Studies for Depositing Highly Dispersed Pt Nanoparticles on Carbon by Use of Trimethyl(Methylcyclopentadienyl)-Platinum(IV) Reactions with O_2 and H_2. *J. Nanopart. Res.* **2015**, *17* (4), No. 179.
(39) Lubers, A. M.; Drake, A. W.; Ludlow, D. J.; Weimer, A. W. Electrochemical Hydrogen Pumping Using a Platinum Catalyst Made in a Fluidized Bed via Atomic Layer Deposition. *Powder Technol.* **2016**, *296*, 72−78.
(40) Goulas, A.; van Ommen, J. R. Atomic Layer Deposition of Platinum Clusters on Titania Nanoparticles at Atmospheric Pressure. *J. Mater. Chem. A* **2013**, *1* (15), 4647−4650.
(41) Grillo, F.; Van Bui, H.; Moulijn, J. A.; Kreutzer, M. T.; van Ommen, J. R. Understanding and Controlling the Aggregative Growth of Platinum Nanoparticles in Atomic Layer Deposition: An Avenue to Size Selection. *J. Phys. Chem. Lett.* **2017**, *8* (5), 975−983.
(42) Mackus, A. J. M.; Weber, M. J.; Thissen, N. F. W.; Garcia-Alonso, D.; Vervuurt, R. H. J.; Assali, S.; Bol, A. A.; Verheijen, M. A.; Kessels, W. M. M. Atomic Layer Deposition of Pd and Pt Nanoparticles for Catalysis: On the Mechanisms of Nanoparticle Formation. *Nanotechnology* **2016**, *27* (3), No. 034001.
(43) Lee, H.-B.-R.; Baeck, S. H.; Jaramillo, T. F.; Bent, S. F. Growth of Pt Nanowires by Atomic Layer Deposition on Highly Ordered Pyrolytic Graphite. *Nano Lett.* **2013**, *13* (2), 457−463.
(44) Lee, H.-B.-R.; Bent, S. F. Microstructure-Dependent Nucleation in Atomic Layer Deposition of Pt on TiO_2. *Chem. Mater.* **2012**, *24* (2), 279−286.
(45) Christensen, S. T.; Elam, J. W.; Lee, B.; Feng, Z.; Bedzyk, M. J.; Hersam, M. C. Nanoscale Structure and Morphology of Atomic Layer Deposition Platinum on $SrTiO_3$ (001). *Chem. Mater.* **2009**, *21* (3), 516−521.
(46) Dameron, A. A.; Pylypenko, S.; Bult, J. B.; Neyerlin, K. C.; Engtrakul, C.; Bochert, C.; Leong, G. J.; Frisco, S. L.; Simpson, L.; Dinh, H. N.; Pivovar, B. Aligned Carbon Nanotube Array Functionalization for Enhanced Atomic Layer Deposition of Platinum Electrocatalysts. *Appl. Surf. Sci.* **2012**, *258* (13), 5212−5221.
(47) Hwang, Y.; Nguyen, B.-M.; Dayeh, S. A. Atomic Layer Deposition of Platinum with Enhanced Nucleation and Coalescence by Trimethylaluminum Pre-Pulsing. *Appl. Phys. Lett.* **2013**, *103* (26), No. 263115.
(48) Pyeon, J. J.; Cho, C. J.; Baek, S.-H.; Kang, C.-Y.; Kim, J.-S.; Jeong, D. S.; Kim, S. K. Control of the Initial Growth in Atomic Layer Deposition of Pt Films by Surface Pretreatment. *Nanotechnology* **2015**, *26* (30), No. 304003.
(49) Grillo, F.; Van Bui, H.; La Zara, D.; Aarnink, A. A. I.; Kovalgin, A. Y.; Kooyman, P.; Kreutzer, M. T.; van Ommen, J. R. From Single Atoms to Nanoparticles: Autocatalysis and Metal Aggregation in Atomic Layer Deposition of Pt on TiO_2 Nanopowder. *Small* **2018**, *14* (23), No. 1800765.
(50) Mackus, A. J. M.; Verheijen, M. A.; Leick, N.; Bol, A. A.; Kessels, W. M. M. Influence of Oxygen Exposure on the Nucleation of Platinum Atomic Layer Deposition: Consequences for Film Growth, Nanopatterning, and Nanoparticle Synthesis. *Chem. Mater.* **2013**, *25* (9), 1905−1911.

https://doi.org/10.1021/acs.jpcc.5c03286
J. Phys. Chem. C 2025, 129, 13822−13829